Statistical Properties of SEE Rate Calculation in the Limits of Large and Small Event Counts

R. Ladbury, *Member, IEEE*

***Abstract*—We develop a Maximum Likelihood method for bounding single-event effect (SEE) rates at a particular confidence level. The method is useful for test planning, reliability estimates and investigating rare SEE modes and part-to-part and lot-to-lot variability.**

***Index Terms*—Quality assurance, radiation effects, reliability estimation.**

I. Introduction

TRADITIONALLY, the treatment of statistical errors in calculation of rates for single-event effects (SEE) has been to minimize them by ensuring that cross sections are estimated with sufficiently large event counts that statistical errors are negligible. The Electronic Industries Association test procedures JESD-57 [1] recommend at least 100 events per data point with possible repetitions at each linear energy transfer (LET) value. Others [2] have gone further, recommending >1000 events for LET values where the cross section is $>5\%$ of the saturated value, >400 events when the cross section is 1%-5% of the saturated value and >4 events near threshold ($<1\%$ of the saturated cross section). Such guidelines ensure that statistical errors are insignificant in rate calculations, especially when the cross section versus LET curve contains several data points.

Unfortunately, achieving such large event counts is not always feasible, especially with destructive SEE mechanisms where each data point may represent the destruction of an expensive microcircuit. In other cases, a disruptive but rare error mode (e.g., a single-event functional interrupt or SEFI) may be discovered only during post-irradiation data analysis, and one must either return to the accelerator for more testing or estimate the error rate for this mode with poor statistics. Having a method for fitting data to a Weibull (or other) curve that takes into account possible Poisson fluctuations on event counts would allow the analyst to bound the SEE rate at any given confidence level. It would also be useful for comparing on-orbit rates (which are usually based on limited statistics) to calculated rates, detecting lot-to-lot or part-to-part variation, test planning and design and many other applications.

Here, we report on a Maximum Likelihood (ML) method for fitting SEE cross section versus LET data to a 4-parameter Weibull. We assume that for the i^{th} LET, LET_i, SEE counts fluctuate according to a Poisson distribution about a mean, μ_i, which is proportional to a cumulative Weibull distribution. We select the fit parameters that maximize the likelihood of our dataset arising due to Poisson fluctuations about the means for each LET. We have implemented the fitting and analysis routines described here as Microsoft Excel™ spreadsheets because Excel is available on most computers and indeed may be the only data analysis program available on SEE test trips. Implementation in Excel allows the analyst to look at the implications of data on the fly and optimize data quality for SEE rate prediction.

Manuscript received July 20, 2007; revised October 2, 2007. This work was supported by NASA's Electronic Parts and Packaging (NEPP) program and the James Webb Space Telescope.

The author is with NASA Goddard Space Flight Center, Greenbelt, MD 20771 USA (e-mail: Raymond.L.Ladbury.1@gsfc.nasa.gov).

Digital Object Identifier 10.1109/TNS.2007.910035

II. Fitting SEE Data and Bounding SEE Rates

When SEE testing yields a null result (that is, no SEE are seen), calculating an upper bound on the SEE rate for a given confidence level is straightforward. One assumes that the 0 events observed represents a downward Poisson fluctuation from the mean at the maximum level allowed by the confidence interval. Thus, at the 95% confidence level, the upper bound for the expected number of events when zero events are observed is 2.9957. (That is, a Poisson distribution with this mean would have a 5% probability of yielding 0 events.) We obtain the cross section by dividing by the ion fluence at the highest LET tested. One can then use a figure-of-merit approach to bound the rate. [3]

When a cross section versus LET curve has several cross section points, bounding the curve for a particular confidence level is more involved. We use a Maximum Likelihood approach. [4] SEE counts, x, are assumed to vary about some mean value μ according to the Poisson distribution

$$P(x,\mu) = \exp(-\mu) \times \frac{\mu^{-x}}{x!}. \tag{1}$$

The mean μ is proportional to the ion fluence, F, and the SEE cross section, σ. The cross section σ is assumed to vary with ion LET according to a cumulative Weibull function with 4 parameters (limiting cross section $\equiv \sigma_{\text{lim}}$, onset LET $\equiv \text{LET}_0$, and Weibull width $\equiv w$, and shape $\equiv s$)

$$\begin{aligned}\mu(\text{LET}_i) &= F_i\sigma \\ &= F_i\sigma_{\text{lim}}\left(1-\exp\left(-\frac{(\text{LET}_i-\text{LET}_0)}{w}\right)^s\right).\end{aligned} \tag{2}$$

We define the likelihood based on Poisson probabilities for our data, $\{\text{x}_i\}$ as

$$\mathcal{L} = \prod_{i=1}^{\text{n}} \text{P}(\text{x}_i,\, \mu = \text{F}_i\sigma_{\text{lim}}\text{W}(\text{LET}_i,\, \text{LET}_{\text{o}},\, \text{w},\, \text{s})) \tag{3}$$

and maximize it with respect to the 4 parameters above (here W is the cumulative Weibull function of the given variables).

TABLE I
SIMULATED SEFI DATA

Effective LET	Cross Section	Events Observed	Effective Fluence
7.80	$0.00\text{x}10^{0}$	0	$1.00\text{x}10^{7}$
11.03	$0.00\text{x}10^{0}$	0	$1.00\text{x}10^{7}$
15.60	$0.00\text{x}10^{0}$	0	$1.00\text{x}10^{7}$
28.80	$1.00\text{x}10^{-7}$	1	$9.99\text{x}10^{6}$
40.73	$6.29\text{x}10^{-6}$	50	$7.95\text{x}10^{6}$
53.10	$2.79\text{x}10^{-5}$	100	$3.59\text{x}10^{6}$
57.60	$4.01\text{x}10^{-5}$	100	$2.50\text{x}10^{6}$
75.09	$1.06\text{x}10^{-4}$	100	$9.46\text{x}10^{5}$
106.20	$2.36\ \text{x}10^{-4}$	100	$4.23\text{x}10^{5}$

W \ S	2.2	2.3	2.4	2.5	2.6	2.7	2.8	2.9
60.0	-67.1	-49.6	-35.7	-24.8	-16.7	-11.2	-7.9	-6.7
62.0	-51.7	-36.2	-24.1	-15.2	-9.0	-5.4	-4.0	-4.7
64.0	-39.0	-25.4	-15.2	-8.2	-3.9	-2.2	-2.7	-5.3
66.0	-28.6	-16.9	-8.6	-3.5	-1.1	-1.3	-3.6	-8.1
68.0	-20.3	-10.5	-4.1	-0.8	-0.3	-2.3	-6.5	-12.8
70.0	-13.9	-5.9	-1.4	0.0	-1.3	-5.1	-11.1	-19.1
72.0	-9.2	-3.1	-0.4	-0.8	-3.9	-9.5	-17.2	-26.9
74.0	-5.9	-1.6	-0.8	-3.0	-7.9	-15.2	-24.6	-36.1
76.0	-4.0	-1.6	-2.5	-6.4	-13.1	-22.1	-33.2	-46.3
78.0	-3.4	-2.7	-5.3	-11.0	-19.3	-30.0	-42.8	-57.5
80.0	-3.8	-4.8	-9.2	-16.6	-26.6	-38.9	-53.3	-69.6

Fig. 1. Log likelihood ratios determine not only the best-fit (black square) parameters for the Weibull fit, but also the confidence intervals for these parameters, as shown for this slice through the 95% confidence contour taken for the best-fit values $\sigma_{\rm lim} = 3.13 \times 10^{-4}$ cm^2 and $\rm LET_0 = 26$.

Because $\mathcal{L}$ is nonlinear in the parameters, we solve the problem numerically by dividing the parameter space for the solution into a grid and calculate the likelihood for the value of $\sigma_{\rm lim}$, $\rm LET_0$, w, and s at each grid point. The routine allows the user to set the starting point and step size for each parameter so that when one is close to a solution one can hone in on the best-fit parameters to arbitrary accuracy. Once an acceptable solution has been determined, one can center on that point and increase the step sizes of the parameters to determine confidence intervals for the parameters and otherwise investigate the behavior of the fit while moving away from the best fit.

As an illustration, consider the idealized data (we use simulated data that fits exactly to a Weibull form to eliminate systematic errors) given in Table I.

We construct the likelihood $\mathcal{L}$ for this data and find our best-fit returns the same parameters that generated the data— $\rm LET_0 = 26$, $\sigma_{\rm lim} = 3.13 \times 10^{-4}$ cm^2, width, $w = 70$ and shape $s = 2.5$ (see Fig. 1). However, as one moves away from the best-fit values $\boldsymbol{\theta_{\rm bf}}$, the likelihood of parameter values $\boldsymbol{\theta}$ is related to the likelihood for $\boldsymbol{\theta_{\rm bf}}$ by

$$\log\left(\frac{\mathcal{L}(\theta)}{\mathcal{L}(\theta_{\rm bf})}\right) \geq -0.5\chi^2(P,k). \tag{4}$$

Here, k is the number of parameters for the fit to the data, and $\chi^2(P,k)$ is the chi-squared statistic for probability P and k degrees of freedom. This makes it possible to define confidence contours as well as best-fit values for the fit parameters. The parameter values that yield the highest SEE rate consistent with a given confidence contour uniquely bound the SEE at the given confidence level for our data.

W \ S	1.3	1.7	2.1	2.5	2.9	3.3	3.7	4.1
30.0	-153.3	-66.1	-30.8	-16.6	-10.9	-8.7	-8.0	-8.0
50.0	-76.6	-24.3	-7.3	-2.0	-0.8	-1.1	-2.1	-3.5
70.0	-47.1	-11.3	-1.7	0.0	-0.8	-2.6	-4.7	-7.1
90.0	-32.2	-6.0	-0.5	-0.8	-2.8	-5.5	-8.4	-11.4
110.0	-23.6	-3.6	-0.7	-2.3	-5.2	-8.5	-12.0	-15.6
130.0	-18.2	-2.6	-1.5	-4.0	-7.5	-11.4	-15.4	-19.4
150.0	-14.6	-2.2	-2.5	-5.7	-9.7	-14.0	-18.3	-22.8
170.0	-12.1	-2.2	-3.5	-7.2	-11.7	-16.3	-21.0	-25.8
190.0	-10.3	-2.4	-4.5	-8.7	-13.5	-18.4	-23.4	-28.5
210.0	-8.9	-2.7	-5.5	-10.1	-15.1	-20.3	-25.6	-30.9

Fig. 2. The same slice of the 95% confidence contour as in Fig. 1, but assuming each SEE cross section is based on only one event.

We facilitate identification of these worst-case parameters by taking the values that yield high figure-of-merit SEE estimators. The figure of merit, [5] FOM, is given by

$$\text{FOM} = \frac{\text{C}\sigma_{\rm lim}}{\text{LET}_{0.25}^2} \tag{5}$$

where C is a constant determined by the radiation environment and $\rm LET_{0.25}$ is the LET where the Weibull reaches 25% of its saturated value:

$$\text{LET}_{0.25} = \text{LET}_0 + w * (0.288)^{1/s}. \tag{6}$$

Although the FOM approach provides a reasonable approximation of the SEE rate, its accuracy varies over the parameter space-especially with onset LET and Weibull shape. For this reason, we use the FOM to identify 10 promising candidates for each confidence interval and then select the parameters that yield the highest SEE rate using the HUP tool from CREME96. [6], [7]

Using the data in Table I and assuming a geostationary orbit, the best-fit rate for a GCR solar minimum environment would be 2.46×10^{-5} SEE day^{-1}, while the 95% CL bounding rate would be 4.11×10^{-5} day^{-1}. Because of the good statistics, the 95% CL rate is only about 67% higher than the best-fit rate.

If instead of the event counts in column 3 of Table I, we had based each cross section on only a single observation of the SEE (as might be the case for an SEL or other destructive test), the confidence contour would be much broader (see Fig. 2). Fig. 3 shows the ratio of the 95% confidence level (CL) bounding rate to the best-fit rate as a function of increasing SEE count for each cross section point (that is, each count being based on 1, 2, 4, 8, 16 and 32 events). As can be seen by the fit to the data, the bounding rate decreases roughly as the inverse of the number of events on which the cross sections are based.

III. SIMULATING EFFECTS OF ERRORS

In addition to the fitting routine described above, we developed a Monte Carlo routine that generated σ versus LET curves from Weibulls with known parameters and allowed the event counts for each cross section point to fluctuate about the mean or expected values according to Poisson statistics. We then fit the

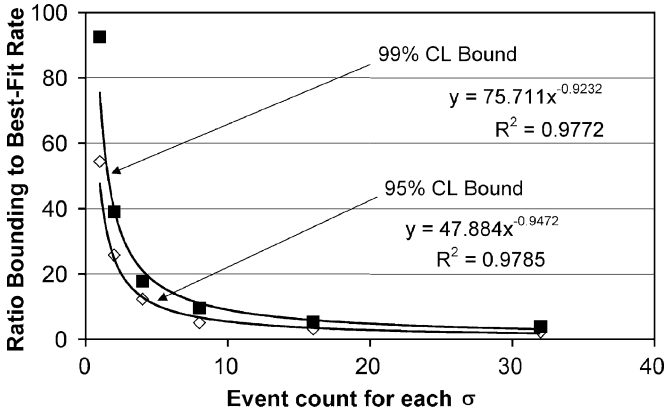

Fig. 3. The 95% CL and 99% CL bounding rates for the simulated data in Table I initially decrease rapidly as the event count for each cross section point increases. Above about 16 events, the decrease is incremental.

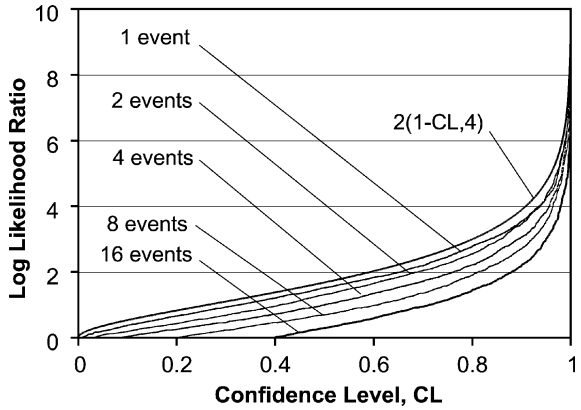

Fig. 4. The logarithm of the ratio of the likelihood for a set of fit parameters to the best-fit parameters tends to scale as the $\chi 2$ statistic with degrees of freedom equal to the number of fit parameters.

TABLE II
SIMULATED SEE DATA

LET (MeV•cm²/mg)	Cross Section
2.8	1.00x10⁻⁷
4.0	1.08x10⁻⁶
5.6	3.32x10⁻⁶
7.8	7.38x10⁻⁶
11.0	1.49x10⁻⁵
15.6	2.78x10⁻⁵
28.8	7.36x10⁻⁵
40.7	1.19x10⁻⁴
53.1	1.64x10⁻⁴
57.6	1.80x10⁻⁴
75.1	2.33x10⁻⁴
106.2	2.99x10⁻⁴

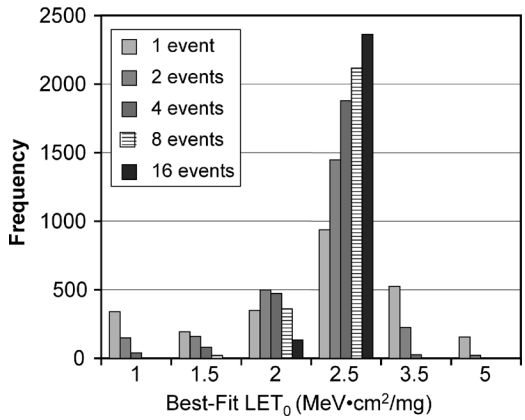

Fig. 5. Onset LET, LET_0, converges rapidly to the correct value as the event count per cross section point increases.

resulting curves and estimated the parameters of the Weibull that generated them. Generating a large number (in our case 2500) of such distributions allows us to determine how Poisson fluctuations affect our ability to determine fit parameters and how this in turn affects our estimates of best-fit and bounding rates. It also allows us to investigate how these errors change as we add additional data or as we change the parameters of our Weibull generating function. Because it is impractical to calculate thousands of rates using CREME96, here we relied more on FOM estimates.

As an example, we discuss in detail a simulated σ versus LET curve generated for a Weibull with $\sigma_{\mathrm{lim}} = 3.58 \times 10^{-4}\mathrm{cm}^2$ $\mathrm{LET}_0 = 2.5$ $\mathrm{MeVcm}^2/\mathrm{mg}$, $w = 70$ and $s = 1.5$. The idealized (Poisson mean) σ values are given in Table II. We initially based each cross section on a single event count and generated 2500 curves (sufficient for estimates good to 2%) with fluctuations. We then fit the curves using our ML technique and looked at how the fit parameters were distributed and how this affected the resulting rate calculation.

We also tested whether (4) above provides a reasonable bound for confidence-level estimates. It is important to test this assumption, because the use of the χ^2 distribution presumes implicitly that errors on the fit parameters are normally distributed. Because of the Poisson nature of errors in SEE counts this cannot be taken for granted.

Fig. 4 shows the distributions of the log of the likelihood ratio for 1, 2, 4, 8 and 16 events per cross section point. Also shown is the χ^2 distribution for 4 degrees of freedom, which does bound the log likelihood ratios. Thus, (4) is appropriate for bounding confidence intervals.

Next, we looked at how event count affects errors on the fit parameters. Fig. 5 shows that the distribution for onset LET from our fitting method narrows rapidly as the event count for each cross section increases. Likewise, the Weibull shape parameter, s also converges well with event count, especially for small s, since this is the range where the shape of the Weibull distribution changes most rapidly with s.

In contrast, cross sections based on small event counts do a poor job pinning down the σ_{lim} and W. Fig. 6 shows that for cross sections based on a single event, the value of σ_{lim} found by the fitting routine can be differ by an order of magnitude from the real value. Moreover, the width of the distribution of σ_{lim} decreases less rapidly than that for LET_0. Errors on the Weibull width are also high for low event counts. However, while the errors on cross section and W are large for small event counts, correlations between these quantities decrease their effect on

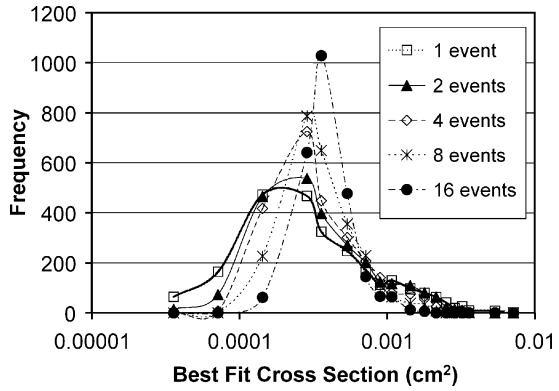

Fig. 6. The limiting cross section, $\sigma\,\mathrm{lim}$, can be off by an order of magnitude or more when points in the σ versus LET curve are based on a single event, and convergence is slow as event count increases.

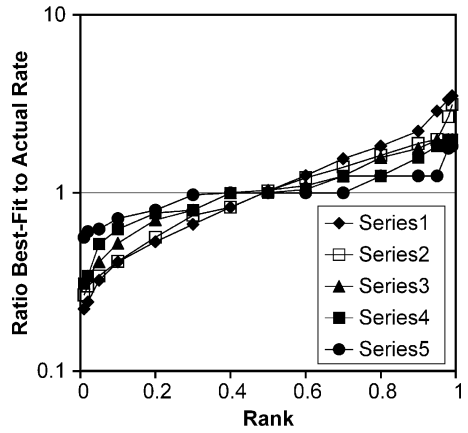

Fig. 8. The ratio of the best-fit rate differs from the actual rate by less than a factor of 5, even when each cross section point is based on only a single event.

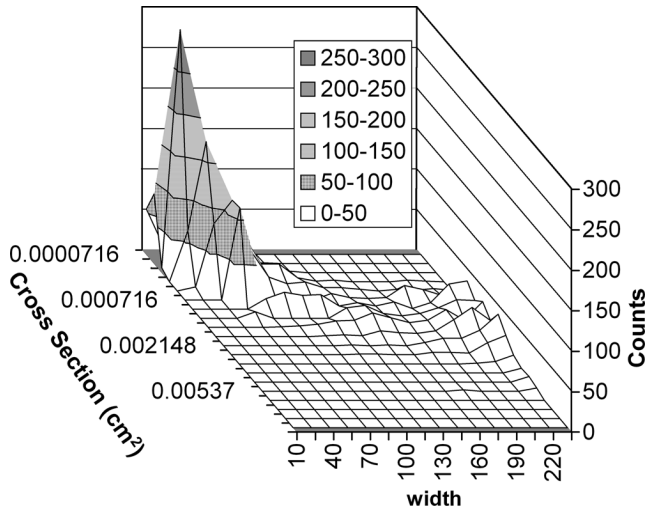

Fig. 7. The limiting cross sections and Weibull width parameters returned by the fitting algorithm tend to be correlated in a manner that decreases errors on SEE rates even when errors on the $\sigma\,\mathrm{lim}$ and w are large. The 3-D scatter plot shown here shows the worst correlation—that for cross sections based on only one event.

TABLE III
CORRELATION BETWEEN σ_{lim} AND w

Event Count, n	Correlation Coefficient
1	0.716
2	0.8
4	0.878
8	0.9
16	0.95

the rate estimation (see Fig. 7). Table III shows the correlation between w and σ_{lim} for increasing event count. This correlation is understandable, since the fit parameters are constrained by the mean trend of the points on the σ versus LET curve.

IV. TEST PLANNING

The foregoing discussion of how statistical errors affect determination of SEE fit parameters and ultimately estimated SEE rates is useful for planning SEE tests as well as for providing guidance to flight projects about interpreting SEE test results. For example, if the data from Table I applied to a destructive SEE, Fig. 3 indicates that bounding the SEE rate to better than $10\times$ could be time consuming and expensive. Alternatively, if the hardware could accommodate the higher bounding rate, testing could be more economical. Thus, the bounding rates can be used in a manner similar to the one-sided tolerance limits for the Parts Characterization Criterion (PCC) hardness assurance methodology [8] for Total Ionizing Dose (TID).

As an example, consider the question of how much the SEE rate for the data in Table II would increase if we only did half as much testing. To investigate this question, we carry out the analysis from Section III again, assuming testing was done only at 6 LETs rather than 12 (that is, keeping the first, third, fifth, seventh, ninth and eleventh data points).

Figs. 9–12 shows how this affects errors (as represented by the standard deviation) on the fit parameters returned by the fitting routine. As expected, halving the number of points in the σ versus LET curve increases the width of the distributions for the fit parameters returned. The effect is most significant for the width parameter, where the initial standard deviation is larger than the value for w that generated the σ versus LET curve. The improvement here is logarithmic with increasing event count, and the rate of improvement for the 12-point curve is much better than that for the 6-point curve. The errors on the other parameters appear to roughly follow a power-law distribution versus event count.

Fig. 13 shows how the trends seen in the fit parameters affect the determination of the expected or average rate for the 99% CL. It is interesting to note that despite the different dependencies of the errors on event count, the dependence of rate on event count follows a simple power law and that it seems to correlate best with the total number of events observed summed over all LET values (that is, the rate for the 12-point curve for n events observed is roughly equal to the rate for the 6-point curve for $2n$ events).

In testing a complex part like an SDRAM, it is important to allocate beam time efficiently. While it is not possible to predict *a priori* what SEE modes a part will exhibit, based on the complicated state machine of the part and past testing of similar parts, we can anticipate that parts will exhibit SEU at very low LET (of

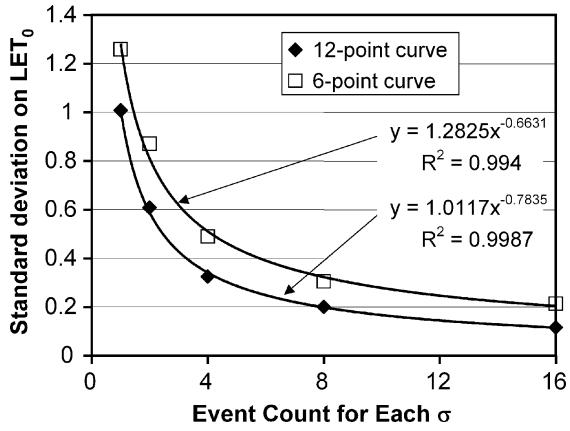

Fig. 9. The standard deviation on the distribution of LET_0 returned by the fitting algorithm starts lower and decreases more rapidly as the number of points in the σ versus LET curve increases.

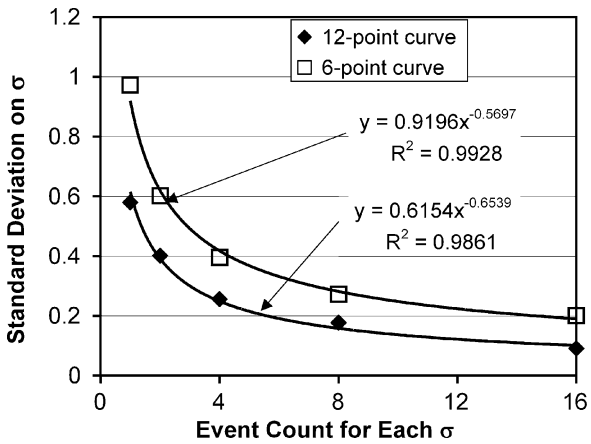

Fig. 10. Standard deviation of the distribution for the Weibull shape returned by the fitting algorithm as a function of event count for 6-point and 12-point σ versus LET curves.

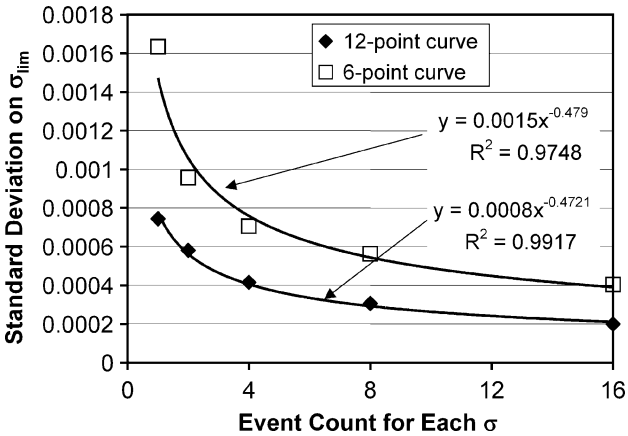

Fig. 11. Standard deviation of the distribution for the limiting cross section returned by the fitting algorithm as a function of event count for 6-point and 12-point σ versus LET curves.

which the curve in Table II might be typical), Multi-bit upsets (MBU) and SEFI at higher LET (perhaps following a curve like that in Table I), and there is a risk of SEL at moderate to high

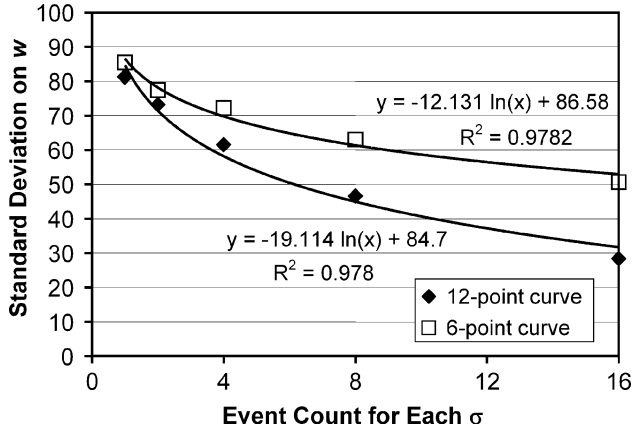

Fig. 12. Standard deviation of the distribution for the Weibull width returned by the fitting algorithm as a function of event count for 6-point and 12-point σ versus LET curves.

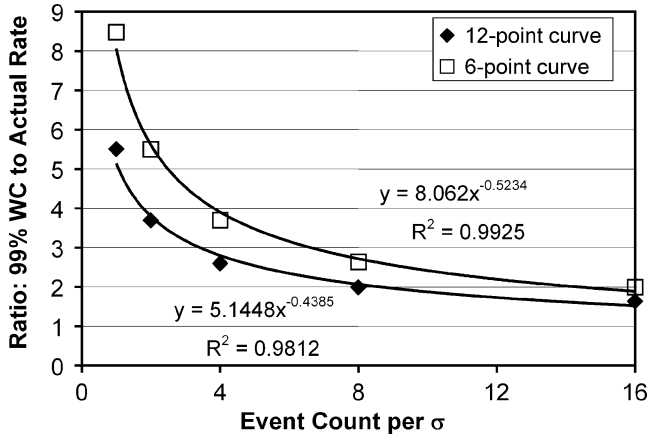

Fig. 13. The expected 99% WC rates for 12-point and 6-point σ versus LET curves as a function of event count per cross section point.

LET. The tools used here allow us to simulate SEE over these LET ranges and with a variety of generating parameters for our idealized Weibulls with a view to optimizing the test plan for rate prediction. Moreover, once we have some data, we can use the same tools to run simulations with lower statistics to make decisions on the fly how to allocate beam time and parts.

V. Part-to-Part and Lot-to-Lot Variability

Because SEE testing is usually not done for every lot, the question of variability in SEE rates—particularly for destructive SEE—is an important and difficult one. The approach outlined here provides significant simplification: If the confidence contours at confidence level α for the two samples overlap, then the disagreement between the two samples is not significant at the level $1 - \alpha$.

Commercial parts are a particular concern when it comes to part-to-part and lot-to-lot variability. BAE Systems carried out a detailed study of such variability in commercial SDRAMs in 2000–2001. Table IV shows data from this study for SEFI in two lots of Hyundai 64 Mbit SDRAMs. Since testing for SEFI is particularly costly, and since sophisticated techniques are required to mitigate SEFI, a finding that lot-specific test data were

TABLE IV
SEFI SUSCEPTIBILITY FOR 2 LOTS OF SDRAMS

LET_{EFF}	σ for lot 1	σ for lot 2	#SEFI lot 1	#SEFI lot 2
2.27	4.8x10^{-8}		1	
7.88	2.7x10^{-7}		1	
7.96		8.8x10^{-7}		6
9.10	3.4x10^{-7}		1	
15.91		2.7x10^{-7}		1
17.80		8.1x10^{-7}		2
22.88		2.8x10^{-6}		7
26.55	3.6x10^{-6}		3	
31.05		2.7x10^{-6}		8
38.03		4.3x10^{-6}		9
41.30	3.3x10^{-6}		1	
53.10	5.6x10^{-6}		2	
53.78		6.9x10^{-6}		19
84.43		8.2x10^{-6}		24
84.71	9.4x10^{-6}		1	

needed to determine SEFI susceptibility could have significant consequences for cost, schedule and design.

The best fits to the two lots are different (Lot 1—$\mathrm{LET}_0 = 0.5$ MeVcm^2/mg, $\sigma_{\mathrm{lim}} = 1.1 \times 10^{-5}$ cm^2, w $= 56$, s $= 1.8$ and corresponding rate 1.1×10^{-5} day^{-1} and Lot 2— $\mathrm{LET}_0 = 0.5$ MeVcm^2/mg, $\sigma_{\mathrm{lim}} = 1.9 \times 10^{-5}$ cm^2, w $= 121$, s $= 1.3$ and corresponding rate 2.24×10^{-5} day^{-1}). However, the 50% confidence contour for each lot overlaps the best-fit parameters for the other lot, so the disagreement is not significant. On the other hand, a similar analysis for MBU, for which statistics are better, does show variation between the lots at a high level of significance.

VI. DIVIDING A DATASET

Often, low statistics in SEE data result from the discovery of a rare error mode that threatens an application and for which the data do not have adequate statistics. This can occur either when the rare mode is discovered in post-processing of a dataset or when the mode comes as a surprise and there is not enough time to gather enough statistics.

An example of the latter occurred during testing of the Analog Devices OP293 op amp for NASA's SWIFT Gamma Ray Burst Telescope. During testing, the OP293 occasionally exhibited very long transients, some lasting on the order of 1 ms. Because these long pulses were rare and time was limited, we accumulated only a small sample of such events.

In subsequent discussions, the project determined that the transients that posed significant concern were those with amplitude over 2 volts and duration over 120 μs. Table V shows the original transient dataset as well as the data for the transients that posed a significant concern.

The data for the long SET amount to only 11 events, so statistical errors are significant. Moreover, the data yield a poor fit to a Weibull and are insensitive to variations in any fit parameter other than σ_{lim}. However, even with the poor fit to a Weibull the data are inconsistent at the 99% CL with any solution yielding a rate higher than 1×10^{-6} day^{-1}.

The fact that the σ versus LET curve gives a poor fit to the assumed Weibull form may mean that systematic errors also contribute to uncertainties in the rate. In our case, because we have taken the worst-case rate consistent with our desired confidence level, the error bars are likely to be larger on the low side than the high side. We consider the issue of systematic errors in the next section.

TABLE V
LONG SET IN THE OP293 OP AMP

LET_{EFF} (MeV•cm^2/mg)	Total SET	Long SET (>120 μs, >2V)	Long SET σ (cm^2)
19.5	751	1	1x10^{-7}
28	525	3	3x10^{-7}
43	679	5	5x10^{-7}
49.5	1303	0	0
87.5	2	2	2x10^{-7}

VII. FUTURE WORK

Although we have concentrated here on the effects of Poisson errors on SEE counts, the techniques discussed here can also be applied to a variety of other problems, including systematic errors and other sources of random error (e.g., part-to-part variability, measurement errors, etc.). One important piece of information we can already glean is the value of the likelihood for the best fit to a Weibull. If the likelihood is significantly lower than would be expected for the number of data points in our curve, this indicates that the data deviate systematically from the expected form (e.g., Weibull). In this case, it is prudent to assume systematic errors contribute more than the usual $2\times$ uncertainty to the rate calculation. One can then combine the contributions of the systematic errors to those of random errors discussed above to ensure that the rate calculated for the part is bounding.

One way to investigate the effects of systematic errors is to generate data that follow a distribution other than a Weibull (e.g., a lognormal or even a Cauchy distribution) and look at the errors that result in the rate. Similar techniques have been discussed previously for investigation of systematic errors in TID hardness assurance. [9] Such studies could be carried out with the routines currently available. Other error types could also be investigated with relatively minor modifications. Candidates include the effects of dead time and contamination of one error mode by another (e.g., contamination of MBU cross sections by SEFI or control errors).

Unfortunately, standard SEE rate calculation packages such as CREME96 do not have the facility to calculate SEE rates based on curve types other than the Weibull, and this complicates analysis of systematic errors based on the form assumed for the cross section. Also, state-of-the-art CMOS technologies often deviate significantly from the assumed rectangular parallelepiped (RPP) charge collection geometry, due to device architecture (especially at low LET) or due to the importance of diffusion-collected charge. While such deviations may require a much more complicated assumed form than the standard Weibull, techniques such as those described here should prove amenable to determining the parameters for the assumed form.

Finally, while the current implementation in Excel is easily portable, some calculations are labor intensive. The current

method should be easy to implement in a stand-alone computer program that can carry out more involved analyses.

VIII. Conclusion

Although the best way of dealing with statistical errors in SEE analysis is to base SEE cross sections on large event counts, this is not always possible. When statistical errors cannot be rendered insignificant, it is important to understand these errors and how they propagate through the rate calculations. This allows us to bound SEE rates in a manner that takes these errors into account. Even where SEE rates are dominated by systematic errors such as departures from the assumed rectangular parallelepiped charge collection or the Weibull form for the cross section versus LET curve, understanding statistical errors facilitates estimation of systematic errors.

The method described here provides an unambiguous way of bounding SEE rates at any given confidence level. Such bounding rates are useful for reliability calculations, for comparison of on-orbit to estimated rates and for comparing estimations from different SEE analysts. Other applications include test planning and optimization, investigations of part-to-part and lot-to-lot variability and rate estimation for rare modes discovered during post analysis of the data.

The techniques described here can be generalized to include systematic as well as random errors. Moreover, the fact that we have used Maximum Likelihood methods means that the technique is amenable to Bayesian analysis if we have archival test data or other information about part performance.

Acknowledgment

The author would like to thank R. Brown of BAE Systems, S. Michalak of Los Alamos National Laboratories, and H. Leidecker of NASA Goddard Space Flight Center for invaluable assistance.

References

[1] "Test procedures for the measurement of single-event effects in semiconductor devices from heavy ion irradiation," Electronic Industries Assoc., Engineering Dept., Arlington, VA, JESD57, 1996.

[2] E. Petersen, "Single-event analysis and prediction," presented at the IEEE NSREC Short Course, Snowmass, CO, 1997.

[3] E. Petersen, "SEE rate calculations using the effective flux approach and a generalized figure of merit approximation," *IEEE Trans. Nucl. Sci.*, vol. 42, no. 6, pp. 1995–2003, Dec. 1995.

[4] P. H. Garthwaite, I. T. Jolliffe, and B. Jones, *Statistical Inference*. London, U.K.: Prentice Hall, 1995.

[5] E. L. Petersen, J. B. Langworthy, and S. E. Diehl, "Suggested single event upset figure of merit," *IEEE Trans. Nucl. Sci.*, vol. NS-30, no. 6, pp. 4533–4539, Dec. 1983.

[6] CREME96 Homepage. 2007 [Online]. Available: https://creme96.nrl.navy.mil

[7] A. J. Tylka *et al.*, "CREME96: A revision of the cosmic ray effects on micro-electronics code," *IEEE Trans. Nucl. Sci.*, vol. 42, no. 6, pp. 2150–2160, Dec. 1997.

[8] R. L. Pease and D. R. Alexander, "Hardness assurance for space systems microelectronics," *Rad. Phys. Chem.*, vol. 43, pp. 191–204, 1994.

[9] R. Ladbury and J. L. Gorelick , "Statistical methods for large flight lots and ultrahigh reliability applications," *IEEE Trans. Nucl. Sci.*, vol. 52, no. 6, pp. 2630–2637, Dec. 2005.